MICROWAVE TRANSPORT IN THE ION-CHANNEL GUIDED FREE-ELECTRON LASER

K.Takayama, J.Kishiro, T.Ozaki, K.Ebihara, S.Hiramatsu
National Laboratory for High Energy Physics in Japan (KEK)
Tsukuba, Ibaraki, 305 Japan

H.Katoh
Dynamic Numerical Simulation Inc. (DYNUS)
2-17-2 Shinyokohama, Kohoku, Kanagawa, 222 Japan

Abstract

Essential features of microwave transport through a plasma filled waveguide were experimentally and theoretically speculated. Reflection and mode-conversion from an oversized RF input-bend and RF(laser) window which substantially reduced an effective input power and amplified power were reproduced in numerical simulations and experimentally confirmed. A 93% transmissible input and output bend which allow a driving beam to pass through the FEL interaction region are proposed.

1. Introduction

Although the single-stage KEK Ion channel giuded X-band Free Electron Laser(IXFEL) driven by electron beams (1.5MeV and 500A) [1-2] has achieved the output power exceeding 30MW at 9.385GHz, microwave amplification in *oversized* RF devices has revealed various undesired features of microwave transport. These features are among RF reflection, mode conversion, a large shot-to-shot jitter(30-40%) in the output power, and RF breakdown on the output RF window which also takes a role of the laser window. Particularly, the reflection and mode conversion at the input RF-bend seen in Fig.1 will disturb the purity of the injected mode(TE_{01}) and degrade its net magnitude available for the amplification. In addition, the reflection and mode conversion at the RF window downstream will largely spoil the FEL amplification itself. The residual plasma electrons between the laser window and the electron beam deflector to keep the UV coated laser window away from direct hitting by energetic electron beams will serve as a resistive and mismatched medium for propagating microwaves.

Main reasons of the above mode conversion can be attributed to the fact that employed RF components such as the input RF-bend, rectangular waveguide, and RF window for RF extraction are notably *oversized.* Use of *oversized* RF components are inevitable in a RF amplifier driven by a low energy beam because, in order to provide a sufficient beam current, the low energy beam occupies a relatively large physical space compared to the driving wavelength in the interaction region. Therefore, a systematic study on the microwave transport through the oversized RF system is really important for optimizing the performance of the current single-stage IXFEL. Ion-channel guiding through the wiggler region has been originally proposed [3], expecting that nonlinear forces

originating from the localized ion channel can introduce tune-spread to lead to BBU suppression in long transport including periodic accelerating gaps. The plasma channel is a source of the plasma electrons of current concern. It is desired to understand effects of the residual plasma electrons on microwave transport in the current IXFEL for further developing this scheme.

Experimental studies of microwaves transport through the plasma channel not associated with FEL amplification were conducted using the set-up seen in Fig.1. A transmission efficiency of microwave power was measured as a function of plasma density. Accordingly, apparent mismatching at an instant when the plasma was generated by the UV excimer laser was observed. A notably fine time-structure of the transmitted microwave pulse over the pulse length was found just below the cutoff plasma frequency. Physical explanations of these features will be given in the next section together with details of the measurement. Characteristics of microwave transport through the RF components of the input RF bends and RF window were independently investigated by using both of MAFIA simulations and real measurement; our concern was mainly focused on reflection and mode conversion at these items as discussed in Section 3. As a result of a series of studies, we realize a type of 93% transmissible input RF-bend with an electron-beam injection open-port of sufficient large aperture to allow the survival of the injected beam current, where 93% of the microwaves injected in TE_{01} mode survives downstream in the same mode. Its detail will be mentioned in the Section 4.

2. Microwave Transport through a Plasma Channel

The test stand consists of a microwave system and a plasma system. The set-up is illustrated in Fig.1.

2.1 Microwave System

The microwave source is a pulsed magnetron operating at 9.385 GHz, capable of nominally generating an output power of 100kW. The microwave signal is converted from the TE_{10} mode to TE_{01} via a tapered waveguide, and fed into an *oversized* rectangular waveguide(WRJ-2, 5.5cm x 11cm) with a input RF-bend, that is, H-bend. The bend corner has an electron beam passing aperture with thin wire mesh. A corner angle of 50° was chosen. The microwave power injected into the 3m-long Rectangular Waveguide (RW) is passed through an output RF window with the function of a laser window where a 15mm thick quartz glass with ε^*=3.78 (for x-band)is embed in a pill-box type cavity, and emitted by a horn antenna in an anechoic room. The receiving small horn is placed 1.8m from the output horn at an angle of 3° from the forward direction, so as not to interfere with a laser beam line. It is noted that the configuration of the receiving horn is suitable for TE_{01}, TE_{03} but not for TE_{02}. The signal is attenuated and detected by a crystal diode, calibrated via thermistor and powermeter. The reflected signal from the lower reaches of the microwave system is coupled out via a directional coupler mounted between the magnetron and the tapered waveguide, attenuated and detected by another crystal diode.

2.2 Plasma System

Diethylaniline (DEA) gas is fed into the beam line including the RW from three reservoir flasks as indicated in Fig.1. The gas pressure is monitored by three Shultz gauge calibrated to a Baratron capacitance manometer, placed at the injector and the RW end. An KrF excimer laser operating at 248nm with 18nsec pulse length is used to ionize the DEA by the two-photon resonant process. Laser pulse energy is measured by a joulemeter and typically is 70mJ/30ϕ, with a shot-to-shot jitter of 3-4mJ. A laser beam was expanded to larger than 50ϕ in diameter so as to occupy the cross-section of the RW. The experiments are performed under the pressure of .1mTorr$\leq$ **P**$\leq$ 3mTorr at the waveguide end. In order to minimize a pressure gradient through the RW, the vacuum line was evacuated via turbo-molecular pumps placing closely to the DEA-gas inlets [4].

A plasma electron density is a key parameter responsible for degraded microwave propagation such as reflection and absorbing. The plasma electron density $n_e(z)$ is known to depend linearly on pressure **P**(z) and quadratically on laser intensity **i**(z);

$$n_e(z) = \alpha \mathbf{P}(z)\mathbf{i}^2(z). \tag{1}$$

where α is the proportional coefficient. The exact values of pressure and laser intensity along the RW were not known except for at both ends. The pressure and the laser intensity at the upper-end of the RW are depicted as functions of the pressure at the lower end in Fig.2. The pressure gradient was small; the difference at both sides was less than 10% in the pressure ranges of .1mTorr-3mTorr. On the other hand, the laser transmission largely depended on the pressure as shown in Fig.2. This is explained by energy loss due to photo-ionization and suggests a spatial variation of the laser intensity along the RW, which is dominated by

$$\frac{d\mathbf{i}(z)}{dz} = W_i\, n_e(z) = \kappa \mathbf{P}(z)\mathbf{i}^2(z) \tag{2}$$

where W_i is the ionization energy of DEA (7eV) and its fragments, and κ is a proportional coefficient involving a geometrical factor and others. Solving Eq.(2), we have the spatial variation of **i**(z),

$$\mathbf{i}(z) = \frac{\mathbf{i}(L)}{-\kappa \mathbf{P}\mathbf{i}(L)(z-L) + 1} \tag{3}$$

where **P**(z)=**P** is assumed and κ is determined by fitting Expression (3) to the experimental data. Using expression (3), the plasma-electron density given by $n_e(z) = \alpha \mathbf{P}\mathbf{i}^2(L)/[-\kappa \mathbf{P}\mathbf{i}(L)(z-L) + 1]^2$ (**i**(L): laser intensity employed in microwave transmission experiments, $70/\pi(1.5)^2$ mJ/cm^2).

2.3 Experiment

In experiments of microwave transmission, the laser was fired almost in the middle of the microwave pulse. Abrupt changes in the transmitted pulse and the reflected pulse were common phenomena synchronized with laser firing. Their characteristic features were identified with the aid of the snapshots of the envelopes of the detected signals presented Fig.3 where 2μsec pulses, with consecutively increasing DEA gas pressure 0.1mTorr<**P**(L)≤3mTorr where L denotes the position in the RW end measured from the reflection corner, are transmitted into the anechoic chamber and reflected at the opposite side. In the low-pressure regions (**P**(L)<.6mTorr) pictured, both signals showed typical mismatching due to the plasma medium filling the waveguide. Beyond .6mTorr the transmitted signal exceeded the peak power of the incident pulse, not accompanied by observable change in the corresponding reflection signal. In the moderate-pressure regions (.7mTorr≤**P**(L)≤1.3mTorr), the mismatching clearly appeared again. In the high-pressure regions (1.3mTorr≤**P**(L)≤2mTorr) below cutoff pressure region (**P**(L)=$\mathbf{P_c}$~3mTorr), both signals manifested the comprehensive fine time-structure. Near the cutoff pressure region (2.4mTorr≤**P**(L)≤$\mathbf{P_c}$), erosion in the transmitted signal and corresponding large reflection were obvious just after laser firing. All of the above phenomena were reproducible within some variation resulted from the shot-to-shot jitter of laser intensity.

2.4 An Idealized Transmission Model

In order to understand qualitatively the experimental results, the following transmission model is exmined. Single mode transmission through a straight *oversized* RW filled, locally in the axial direction and uniformly over the cross-section, with mismatched mediums of the plasma electrons and the dielectric material with ε^*=3.78 is considered. This is in real justified since TE_{01} and TE_{03} modes dominate the received transmitted-signal as mentioned in the previous sub-section; meanwhile, the picked-up reflection signal is not the case because higher modes such as TE_{02} converted from the incident TE_{01} mode may be contained. Assumed that the time scale for the variation of the plasma-electron density is much longer than microwave's transit time $L/v_p \sim L/c$, spatial evolution of the TE_{mn} mode through the RW (a×b) is written by the following wave equation,

$$\frac{\partial^2 \mathbf{E}}{\partial z^2} + \left\{k_0^2(z,t) - \left(\frac{m\pi}{a}\right)^2 - \left(\frac{n\pi}{b}\right)^2\right\}\mathbf{E} = 0 \qquad (4)$$

where $k_0^2(z,t)=(\omega/c)^2$ in vacuum or open air, $(\omega/c)^2[1-(\omega_p(z,t)/\omega)^2]$ in plasma-channel, $(\omega/c)^2\varepsilon^*$ in window. $\omega_p(z,t)$ $(\equiv\sqrt{e^2\mathbf{n_e}(z,t)/m\varepsilon_0})$ is the plasma frequency and a cutoff plasma-electron density is given by $\mathbf{n_c}=(m\varepsilon_0/e^2)[\omega^2 - (\pi nc/b)^2]$ for TE_{0n} mode ($9.86\times10^{11}/cm^3$ for TE_{01} mode and $2.59\times10^{11}/cm^3$ for TE_{03} mode at $\omega/2\pi$=9.385 GHz). Here the collision frequency ν_c is not included in the analysis

because of $\omega >> \nu_c$ in the parameter regions of interest here. The plasma electron density is a time-varying function which is dominated by the rate-equation,

$$\frac{\partial n_e}{\partial t} = \nu_i n_e - \alpha_r n_e^2 - \nu_D n_e \qquad (5)$$

where ν_i is the ionization frequency, α_r is the recombination coefficient and ν_D is the diffusion frequency. Since ν_i and ν_D are assumed to be negligibly small from reasons described in Ref.[6], the solution of Eq.(5) is written by $n_e(z,t)=1/[(1/n_e(z,0)) + \alpha_r t]$. Although there have been no reliable reports of the recombination coefficient for DEA and its fragments, Loeb and Biondi [9] have suggested $\alpha_r=10^{-8}$-10^{-6} (cm^{-3}/s) for many molecules. For the e^--density close to n_c, a large decay is estimated at $\alpha_r=10^{-6}(cm^{-3}/s)$.

It is possible to analytically evaluate the transmission efficiency introducing the above expression $n_e(z,t)$ into Eq.(4) where the varying wavenumber involves an inverse quadratic-term of z, as depicted in Fig.4. The solution of Eq.(5) in the region with a constant wave-number is trivial. The solution for a finite time in the plasma-filled region is given in a form of WKB solution. Amplitudes of the forward and backward-waves can be algebraically calculated from the continuity of the electro-magnetic fields at the boudaries. Eventually, we obtain the transmission efficiency $|T|^2$ as a function of time for an initially assumed pressure.

This value for TE01 mode just after laser firing is shown in Fig.5a. The feature of oscillatory decreasing of $|T|^2$ with pressure seems to be consistent with the experimental result. This is unique in the case with a gradient wave-number; the characteristics is not observed in other cases such as the transport-line with a step function-like wave-number. The temporal evolution of $|T|^2$ is plotted for two different extreme cases of α_r in Fig.5b. In the high pressure region, substantial recovery of the transmission efficiency with time is obvious for the case of $\alpha_r = 10^{-6}cm^3sec$. The feature is understandable from a simple speculation that the gradient in the electron density rapidly disappears. However, the analytic feature of the transmission model at least qualitatively disagrees with the experimental result (erosion) that the transmission decreases in a large scale of time. Thus, the large magnitude of α_r is ruled out. On the other hand, the case of the small α_r ($=10^{-8}/cm^3sec$) fails to reproduce the spiky-recovery of transmission which is another notable characteristics of the experimental results.

From the above considerations, it turns out that the current theoretical transmission model is insufficient to explain the whole aspects of experimental results. Nature may require a more novel model. It seems to be worth examining a speculation that the ponderomotive forces created from the coupling between

the forward and backward waves induces the redistribution of the plasma electrons in the longitudinal direction and a periodic structure is formed with time-constant of interest. The abnormal recovery of the transmitted power with no notable-change in the reflected signal near **P**(L)≅.6mTorr is still not explained. It will be attributed to any other mechanism such as a reduction of mode conversion from incident TE_{01} to TE_{02} which will be discussed in the next section.

3. Reflection and Mode Conversion at Oversized RF Components

Possible sources of the reflection and the mode-conversion in the RF system without the residual plasma are the *oversized* input RF-bend and *oversized* RF window. Two sorts of input bend, that is, E-bend and H-bend with almost 45° reflection corner as seen in Fig.6 have been tried in the FEL amplification experiments. There were no notable differences in the FEL amplification performance. Maximized power fraction which can reach to the receiver horn was always limited to less than 30kW even when full-power injection. For the purpose to identify quantitatively the reflection and the mode-conversion taking place at each of the RF components, MAFIA simulations were performed. Typical results are listed in Fig.7 in a form of fractional ratio. Their characteristics are summarized as follows,

--- Large fractions are converted to TM modes in the E-bend.
--- Converted modes are limited to TE modes, particularly TE02 and TE_{03}, in the H-bend.
--- Reflecting power is 15-20% of the incident one for both bends.
--- These features strongly depend on the reflection corner-angle (not shown here, chosen examples have a maximized efficiency).
--- Window thickness is a parameter to determine the reflection. The case (d(thickness)=λ(wavelength in the window)=1.63cm) minimizes the reflection, yielding a few%.

To confirm a part of predictions by simulation works, TE_{02} and TE_{03} modes converted from the incident TE_{01} mode at the H-bend were experimentally observed. Under the similar set-up to that in Section 2, the transmitted power was monitored, moving the receiver horn in the vertical direction. The received power is mixing of TE_{01}, TE_{02} and TE_{03} and in Fig.8 is plotted in an arbitrary unit as a function of vertical height measured from the center of the RW. Asymmetry of the power density in the vertical direction is remarkable. This suggests that the mode-conversion in the input RF-bend, particularly into TE_{02}, is really serious and is consistent with the simulation results. The injected microwave for FEL amplification is very far from an ideal plain-wave.

4. 93% Transmissible Oversized Input and Output RF-bend

Minimizing the reflection and the mode-conversion in the input RF-bend is desired without doubt. There is no simple technique to determine a physical configuration of the *oversized* input bend so as to do so. Extensive knowledges of a basic-size waveguide with respect to *bend* are of no use. However, it is possible to optimize the physical dimension by aid of simulation codes and a so-

called mode-coupling theory [10] under some general strategy such as smooth modification of the metal boundary. As an example, a H-bend as shown in Fig.9 is presented, which demonstrates 99% power transmission(see H-bend(B) in Fig.7) without the beam passing port and 93% power transmission with an open beam-port of 20mm in diameter. The latter is a practical candidate in the coming stage, because the metal corner-mesh always degrades a driving beam quality, that is, the brightness. A fraction (3%) of the missing power is the reflection and the rest is brought out in TE_{11} mode propagating through the beam port.

Using this sort of input-bend in the reverse way, it works as an output RF-bend which allows a driving beam to enter into the next amplification stage without disturbed and the extracted microwave power to be introduced into desired applications. A RF window developed only for its purpose will be available there.

5. Conclusion and Perspective

From a microwave-transport point of view, we have investigated various undesired aspects in the KEK-IXFEL and tried to manifest their reasons. We have found the transmissible power in TE_{01} mode is limited to 30% of the injected magnitude due to mode conversion and reflection at the input RF-bend and reflection at the RF window. it was shown by a systematic experimental study that the residual plasma seriously affects the microwave transport in the high density regions. A theoretical transmission model to understand the experimental results was proposed but it turned out that the idealized model is not enough to fully explain the experimental results. For further developing the model, experimental measurements of key parameters of the diffusion coefficient of the plasma electrons and their recombination coefficient with DEA and its fragments under microwaves of 100kW level will be indispensable. In addition, transmission test avoiding the mode conversion should be done using a very low power which substantially reduces the disturbance on the electron-density as pointed out in Sec.2.4 .

To realize a travelling-wave amplifier in the multi-stage scheme capable operated in an engineering level beyond the R&D stage, all of issues must be overcome. A early study [11] has shown that a large seed-power exceeding 10MW at Ka-band is required for stabilization of the output-phase variation due to beam jitter. Power loss at the injection must be minimized. The new input RF-bend presented here will meet such requirement.

Acknowledgements

The authors wish to thank Director of Accelerator Department Prof. Y. Kimura for his continuous support to our R&D works. The late Prof. K. Narushima gave helpful suggestions to our vacuum system. They thank D.Arakawa, Y.Ohsawa, K.Saito, S.Hashimoto, H.Hisamatsu, and D.Whittum for providing useful suggestions and helpful asistances during setting-up and calibrating the experimental devices.

References

[1] T.Ozaki, K.Ebihara, S.Hiramatsu, Y.Kimura, J.Kishiro, T.Monaka, K.Takayama and D.Whittum, *Nucl. Inst. and Meth.* **A318**, 101 (1992).
T.Monaka, Doctoral Thesis, to be published.

[2] S.Hiramatsu, K.Ebihara, Y.Kimura, J.Kishiro, T.Monaka, T.Ozaki, K.Saito, K. Takayama and D.H.Whittum, *Nucl. Inst. and Meth.* **A331**, 113 (1993).
J.Kishiro et al., 1993 Accel. Conf. in Washington, to be published in Proc..

[3] K.Takayama and S.Hiramatsu, *Phys. Rev.* **A37**, 173 (1988).

[4] K.Narushima, private communication (1992).

[5] K. Takayama, *Phys. Rev.* **A45**, 2618 (1992).

[6]Electron impact ionization cross-sections of DEA and its fragments is not available in the wide range of electron beam energy. The plasma electrons are known to have almost a δ-function like distribution in momentum space just after laser firing (E=3eV) [7]. The input power of 100kW results in the peak electric-field strength of 2 kV/cm to give the averaged kinetic energy of .3eV. Expanding of plasma electrons in momentum space due to collision is negligible small during the pulse because of $\nu_c << \omega$. It is unlikely for plasma electrons to get a sufficient kinetic energy to ionize these molecules (W_i =7eV). Thus, $\nu_i \approx 0$. The diffusion frequency for free electrons is given by $\nu_D = D\pi^2/a^2$ from the boundary condition $\mathbf{n}(0,t) = \mathbf{n}(a,t) = 0$ where the diffusion coefficient, D, follows the empirical relation $D \bullet \mathbf{P}(\text{Torr}) = 5\times10^5 \text{cm}^2/\text{sec}$ [8]. Substitution of a = 5.5cm gives $\nu_D = 1.65\times10^5/\mathbf{P}(\text{Torr})\ \text{sec}^{-1}$. Substitution of **P**=0.1mTorr in the lower pressure region of the present experiment into the expression leads to an extremely large diffusion frequency. However, the experiments in this pressure region didn't indicate a rapid recovery of the transmission easily expected from such decay of the plasma electrons during the pulse length, as seen in Fig.3. The above diffusion coefficient may be not suitable in the present situation. It should be significantly affected by plasma-electron confinement due to ponderomotive forces which are generated by microwaves with spatial variation.

[7] M.D.Perry and O.L.Landen, *Phys. Rev.* **A38**, 2815 (1988).

[8] A.D.MacDonald, in Microwave Breakdown in Gases (John Wiley & Sons, Inc. New York, 1966), 26.

[9] L.B.Loeb, in Handbuch der Physik, 471 (1956).
M.A.Biondi, *Phys. Rev.* **129**, 1181 (1963).

[10] K.Katoh, T.Kikunaga, T.Ozaki, and K.Takayama, preparing for publication.

[11] K.Takayama, *Part. Accel.* **39**, 65 (1992).

Figure Captions

Fig.1 Experimental set-up.
Fig.2 Laser transmission vs. pressure **P**.
Laser intensity was monitored at the corner of input RF-bend and the input laser power was $\mathbf{i}(L)=24.2/\pi$ mJ/cm^2. Broken line is the best fitted curve of $\pi\mathbf{i}(0)$.
Fig.3 Microwave transmission and reflection vs. pressure **P**.
Top and bottom lines show the transmitted and reflected signals, respectively.
Fig.4 Varying wavenumber along the transmission line
Fig.5a Theoretical transmission efficiency vs. pressure just after the laser timing
Fig.5b Temporal evolution of theoretical transmission efficiency for different pressure **P**.
Thin solid line: $a_t=10^{-6}$/cm^{3}sec, thick solid line: $a_t=10^{-8}$/cm^{3}sec.
Fig.6 E-bend, H-bend with 45° reflection corner angle, and RF-window.
Fig.7 Simulation results on transmission, reflection, and mode-conversion.
Fig.8 Vertical variation of experimentally received power.
Fig.9 Side view of the 93% transmissible H-bend.

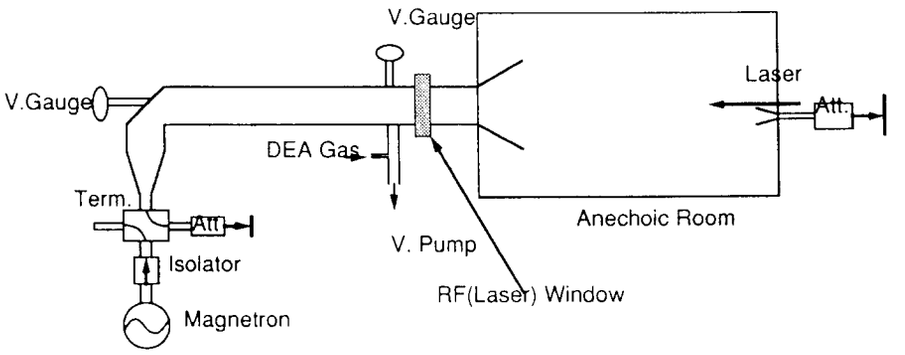
V.Gauge
V.Gauge
Laser
Att.
DEA Gas
Term.
Att.
Anechoic Room
V. Pump
Isolator
RF(Laser) Window
Magnetron

Fig. 1

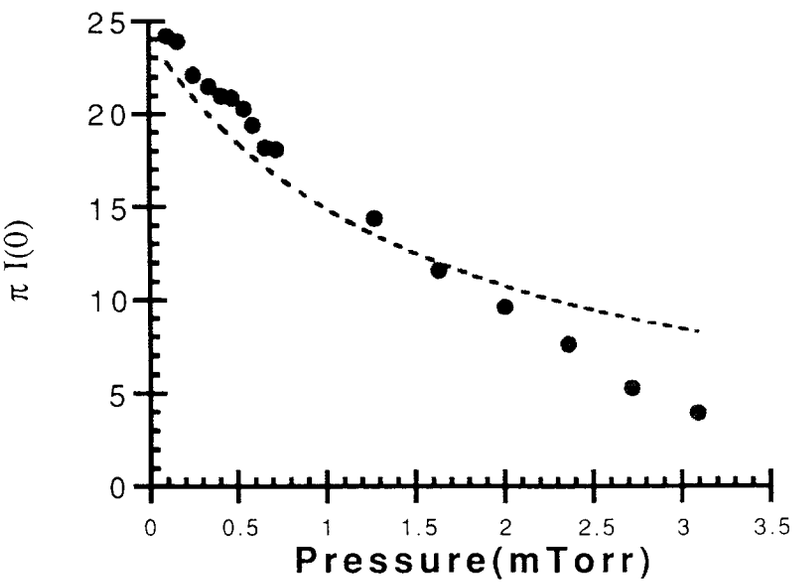
25
20
15
10
5
0
π I(0)
0
0.5
1
1.5
2
2.5
3
3.5
Pressure(mTorr)

Fig. 2

P=.16 mTorr

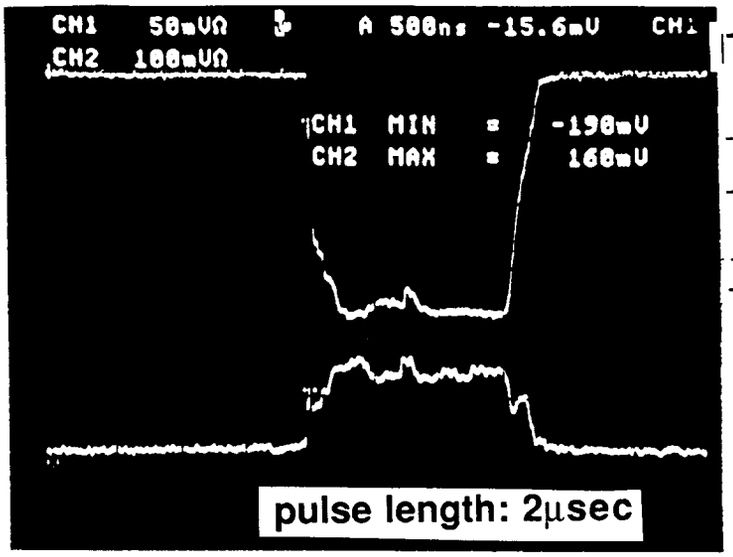

P=1.3 mTorr

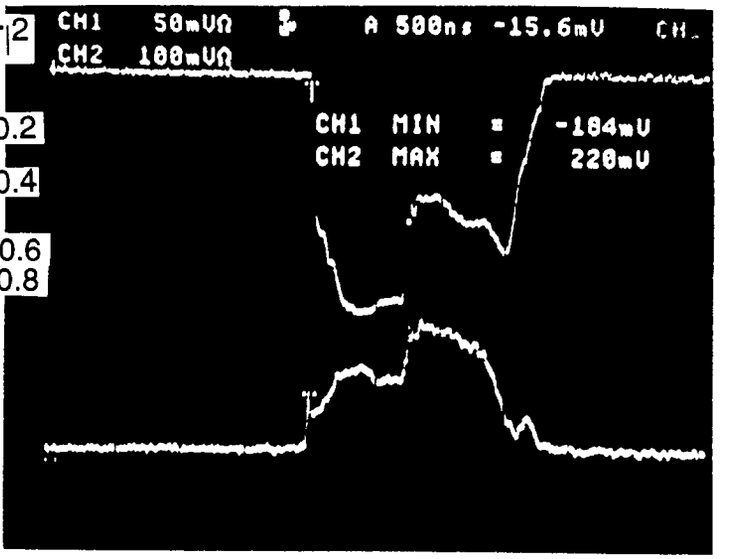

$|T|^2$

-0.2

-0.4

-0.6

-0.8

P=.34 mTorr

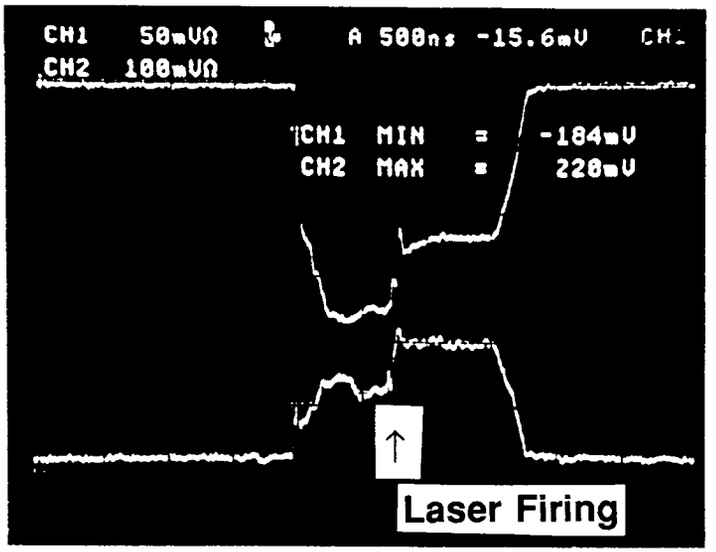

P=1.6 mTorr

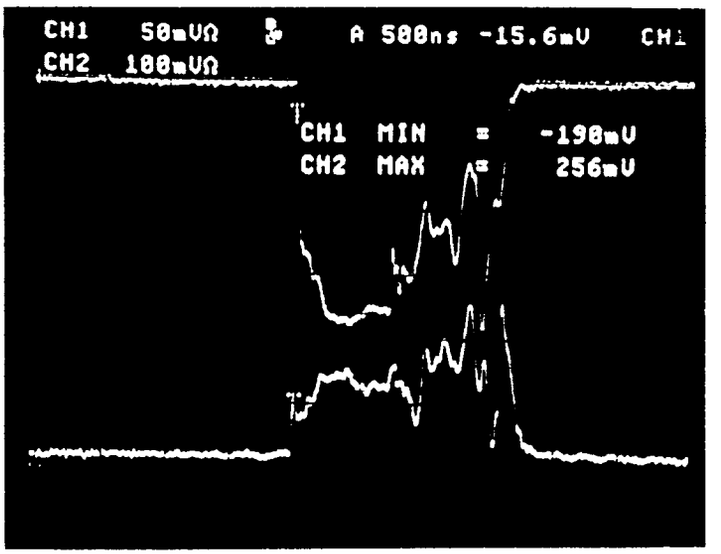

P=.54 mTorr

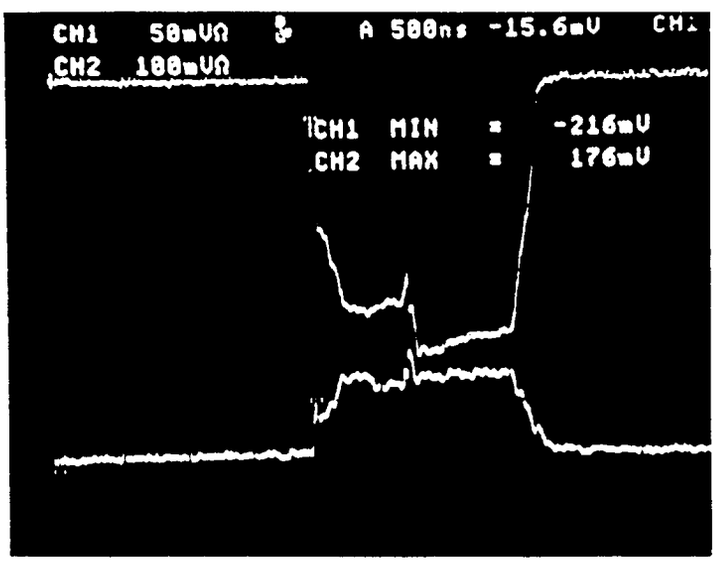

p=2.7 mTorr

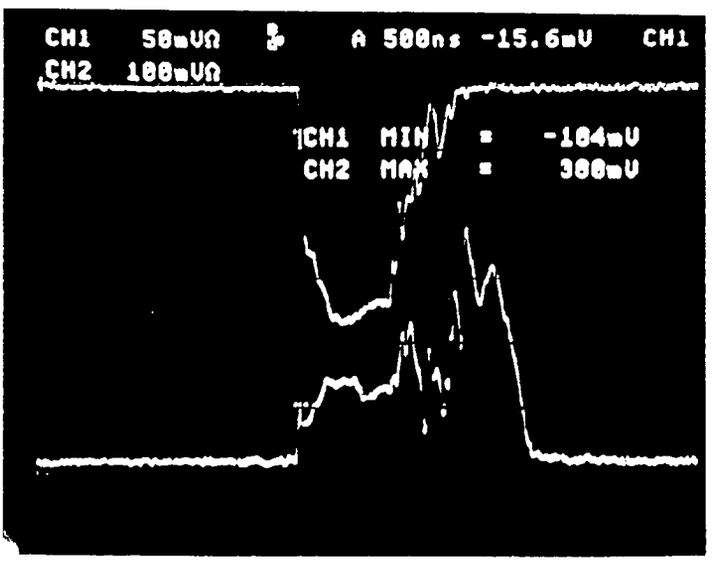

Fig. 3

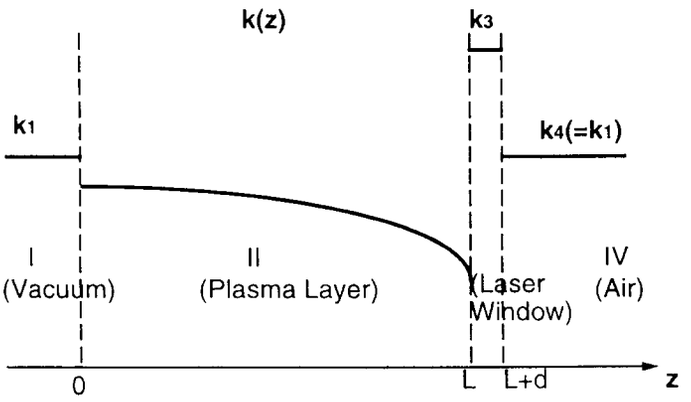

Fig. 4

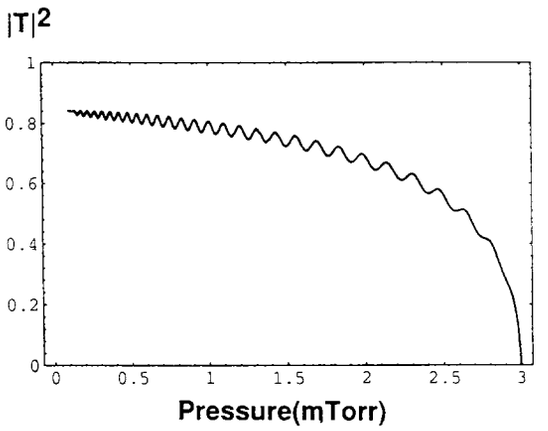

Fig. 5a

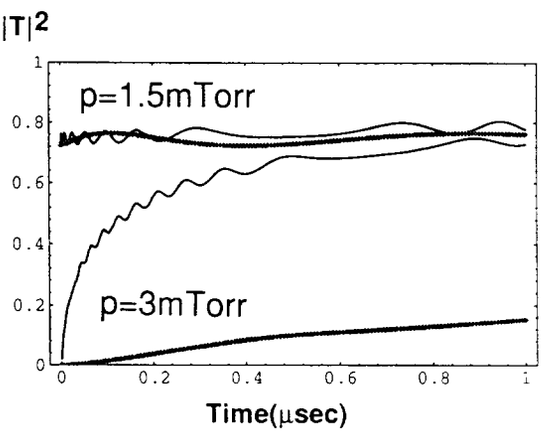

Fig. 5b

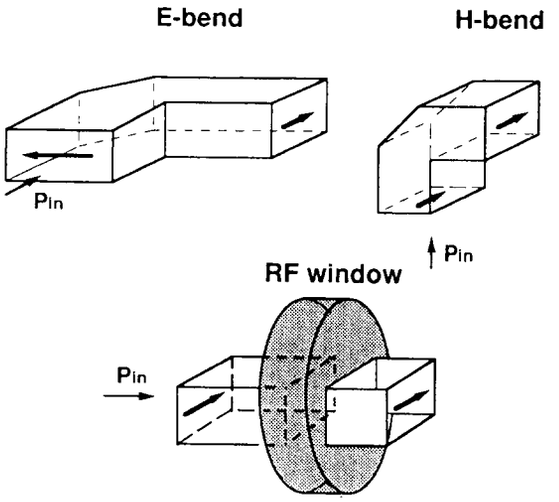
E-bend
H-bend
Pin
Pin
RF window
Pin

Fig. 6

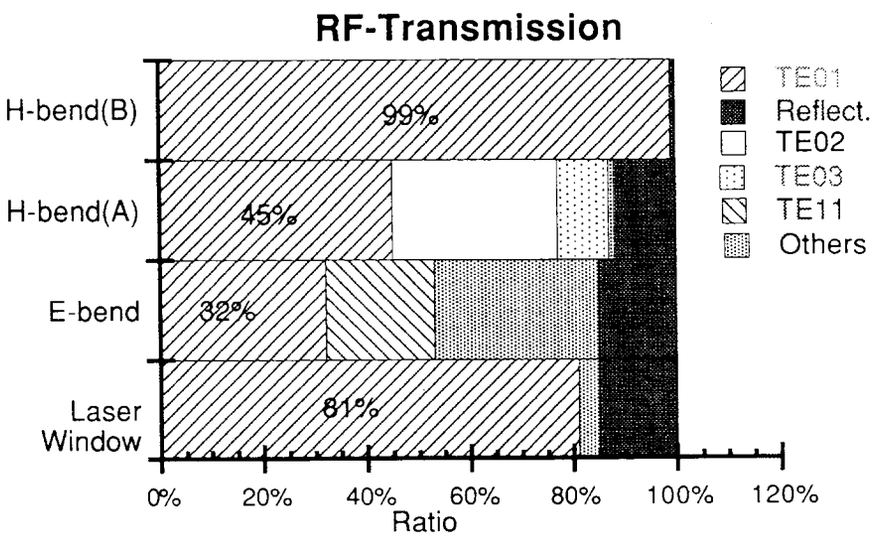
RF-Transmission
H-bend(B)
H-bend(A)
E-bend
Laser Window
99%
45%
32%
81%
TE01
Reflect.
TE02
TE03
TE11
Others
0%
20%
40%
60%
80%
100%
120%
Ratio

Fig. 7

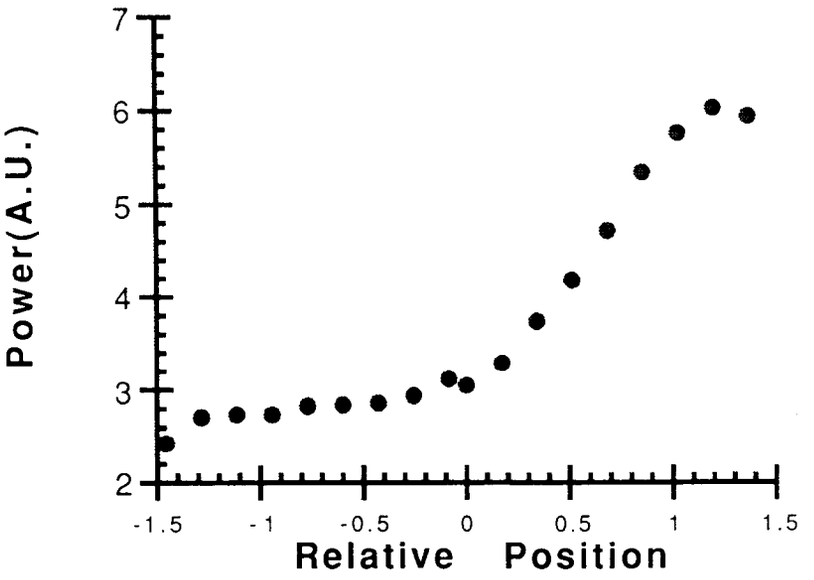
Power(A.U.)
7
6
5
4
3
2
-1.5
-1
-0.5
0
0.5
1
1.5
Relative Position

Fig. 8

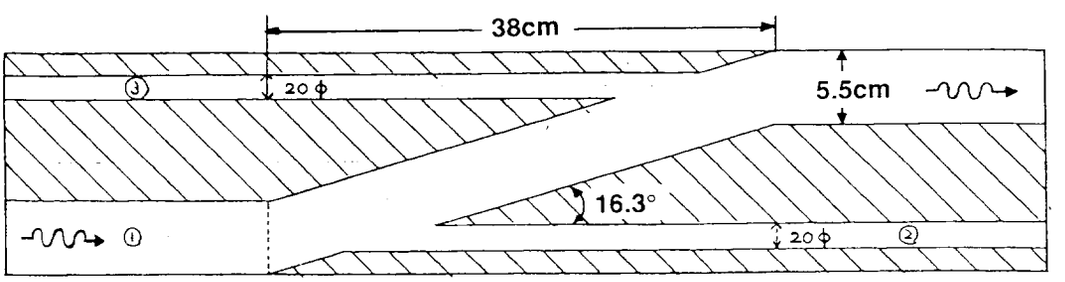
38cm
③
20 ϕ
5.5cm
16.3°
①
20 ϕ
②

Fig. 9